PROCEEDINGS, Thirteenth Workshop on Geothermal Reservoir Engineering
Stanford University, Stanford, California, January 19-21, 1988
SGP-TR-113

SOME EFFECTS OF NON-CONDENSIBLE GAS IN GEOTHERMAL RESERVOIRS WITH STEAM-WATER COUNTERFLOW

Robert McKibbin* and Karsten Pruess

Earth Sciences Division, Lawrence Berkeley Laboratory,
University of California, Berkeley, California 94720

ABSTRACT

A mathematical model is developed for fluid and heat flow in two-phase geothermal reservoirs containing non-condensible gas (CO_2). Vertical profiles of temperature, pressures and phase saturations in steady-state conditions are obtained by numerically integrating the coupled ordinary differential equations describing conservation of water, CO_2, and energy. Solutions including binary diffusion effects in the gas phase are generated for cases with net mass throughflow as well as for balanced liquid-vapor counterflow. Calculated examples illustrate some fundamental characteristics of two-phase heat transmission systems with non-condensible gas.

INTRODUCTION

It is well established that a mechanism of gas-liquid counterflow, also known as a "heat pipe," provides the main heat transfer in two-phase reservoirs of vapor- and liquid-dominated type (White et al., 1971; Martin et al., 1976; Straus and Schubert, 1981; Pruess, 1985; Iglesias et al., 1986; Pruess et al., 1987; McGuiness and Pruess, 1987; and others).

A heat pipe is here supposed to be a steady-state mechanism established in a porous medium where heat is transferred by a process of vapor rising vertically from depth to condense near the top with the liquid condensate moving under gravity downwards in counterflow to the rising gas. Additional heat transfer also occurs by conduction. There may be a net flow of mass through the system, although many of the previous studies assume this is negligible, or zero.

Previous work on heat pipe conditions in geothermal reservoirs has been restricted to the consideration of two-phase single-component flow of liquid water and vapor. However, many two-phase reservoirs contain considerable amounts of non-condensible gases, chiefly CO_2. The CO_2 content of the produced geofluids is often in the range of 0.1 - 10% and in some cases is much higher. The initial composition of the produced fluid in the Bagnore field in Italy was greater than 80% by weight CO_2 (Atkinson et al., 1980). The Broadlands geothermal field in New Zealand contained about 4% by mass CO_2 in the fluid before exploitation (Sutton and McNab, 1977). During initial production from such fields, the CO_2 content of the produced fluid is much higher than *in situ* values, and the reservoir appears to degas quickly (O'Sullivan et al., 1985). Surface manifestations in geothermal fields are also often rich in CO_2.

Studies in the heat transfer literature have indicated that the presence of non-condensible gas can have strong effects on heat pipes. The non-condensible gas tends to accumulate near the cold (condensing) end of the heat pipe, where molecular diffusion is balanced by mass convection; this accumulation reduces the effective heat pipe length (Udell and Fitch, 1985). The quantitative details of non-condensible gas concentration near the cold end of a heat pipe depend on the strength of binary diffusion between the non-condensible gas and the vapor. This strength is, apart from pressure and temperature, a function of formation tortuosity and volumetric gas phase content. Thus, from observed profiles of CO_2 concentrations versus depth it should be possible, at least in principle, to obtain some insight into gas phase saturation in a geothermal reservoir.

In this paper a model for steady-state vertical gravity-driven heat pipes containing water and CO_2 is developed. Mathematically, the model is represented by three coupled ordinary differential equations which express conservation of mass of water, mass of CO_2 and energy, respectively. Numerical integration of these equations gives vertical profiles for temperature, pressures, phase saturations and phase compositions for heat pipes with and without net mass throughflow. The profiles are compared with those calculated by numerical simulation of transient heat pipe conditions using the program MULKOM (Pruess, 1983).

The results indicate that, with or without a net mass throughflow, the partial pressure of any non-condensible gas present in the heat pipe forms a characteristic "wedge" at the top. Within this "wedge," there is very little fluid movement, with the main condensation region for the heat-pipe counterflow occurring at the bottom, or tip, of the "wedge." Above this condensing zone, temperature gradients are close to conductive. The gas zone therefore appears to act as a transition region between the heat pipe and a conduction zone of low permeability above.

For a net CO_2 mass flow through the system, partial pressures of non-condensible gas are non-zero at depth, and there is a simple relationship between the partial pressure and net mass flowrate per unit area of CO_2. For a zero net throughflow, the partial pressure of CO_2 is negligible at depth.

*On leave from Geothermal Institute, University of Auckland, Private Bag, Auckland, New Zealand

The inverse problem of trying to determine relative permeabilities and phase saturations from observed pressure and temperature profiles in a reservoir is also studied. The accuracy needed in temperature and pressure measurements to provide good estimates of the flow parameters is estimated.

MATHEMATICAL MODEL

The heat pipe is supposed to consist of steady vertical flows or a counterflow of liquid and gas, with two components, namely water and CO_2, within a porous matrix. Binary diffusion may occur in the gas phase of vapor and gaseous CO_2. The liquid phase consists of water and dissolved CO_2. Thermal equilibrium at each point is assumed, i.e., the temperature of liquid, gas and matrix are the same at each point in the system. Capillary pressure is neglected, i.e. $p_l = p_g = p_v + p_c = p$. The partial pressure of CO_2 gas and the mass fraction of dissolved CO_2 in the liquid phase are related by Henry's law.

Using conservation of momentum (Darcy's law), the mass flow rates per unit area in the z-direction (the z-axis is positive vertically upwards) can be written as follows:

(i) for water:

$$F_l^w = -(1-X)\frac{k k_{rl}}{\nu_l}\left(\frac{dp}{dz} + \rho_l g\right), \tag{1}$$

$$F_g^w = -(1-Y)\frac{k k_{rg}}{\nu_g}\left(\frac{dp}{dz} + \rho_g g\right) - \rho_g \tau \phi S_g D_{vc}\frac{d(1-Y)}{dz}; \tag{2}$$

(ii) for CO_2:

$$F_l^c = -X\frac{k k_{rl}}{\nu_l}\left(\frac{dp}{dz} + \rho_l g\right), \tag{3}$$

$$F_g^c = -Y\frac{k k_{rg}}{\nu_g}\left(\frac{dp}{dz} + \rho_g g\right) - \rho_g \tau \phi S_g D_{vc}\frac{dY}{dz}, \tag{4}$$

where X and Y are the mass fractions of CO_2 in the liquid and gas phases, respectively. The liquid and total gas pressures are equal, i.e., $p = p_v + p_c$, where $p_v = p_{sat}(T)$ is the saturation pressure corresponding to the local temperature and p_c, the partial pressure of the CO_2 gas, is related to the CO_2 liquid mass fraction X by Henry's law. Since X is small, this relationship can be written, to good accuracy, as

$$p_c = K_H X \frac{M_{H_2O}}{M_{CO_2}}$$

where K_H, a function of temperature, is Henry's constant. The binary diffusion coefficient D_{vc} is written as (Perry, 1963)

$$D_{vc} = D_{vc}^0 \frac{p_0}{p}\left(\frac{T + 273.15}{273.15}\right)^{\theta}$$

where $D_{vc}^0 = 1.38 \times 10^{-5}$ m^2/s (for standard conditions of $p_0 = 1$ bar, $T = 0\,^\circ$C) and $\theta = 1.91$.

Application of the principles of conservation of mass of water, mass of CO_2, and heat flow in the z-direction lead to the equations

$$F_l^w + F_g^w = m_w \tag{5}$$

$$F_l^c + F_g^c = m_c \tag{6}$$

$$F_l^w h_l^w + F_g^w h_g^w + F_l^c h_l^c + F_g^c h_g^c - K\frac{dT}{dz} = q \tag{7}$$

where m_w, m_c and q are constant water mass flow rate, CO_2 mass flow rate and heat flux, respectively, all per unit cross-sectional area.

By substituting the expressions (1) - (4) for the mass flow rates into (5) - (7), writing $p = p_v + p_c$ and using the Clapeyron equation, the Equations (5) - (7) become a set of three coupled first-order ordinary differential equations for T and p_c, with coefficients that depend on T, p_c and S_g (the volumetric gas saturation). The thermodynamic properties of water and CO_2 are calculated from correlations as used by O'Sullivan et al. (1985). Thus (5) - (7) are of the form

$$a_{i1}\frac{dT}{dz} + a_{i2}\frac{dp_c}{dz} = b_i, \quad i = 1, 2, 3,$$

where the a_{ij} and b_i are functions of T, p_c and S_g. For given values of T and p_c, the condition that this set of equations be consistent is

$$\det\begin{bmatrix} a_{11} & a_{12} & b_1 \\ a_{21} & a_{22} & b_2 \\ a_{31} & a_{32} & b_3 \end{bmatrix} = 0$$

which gives an equation to be solved for S_g. Once S_g is determined, dT/dz and dp_c/dz can be found.

The coefficients a_{ij} and b_i also depend on the parameters K, k, τ, ϕ, q, m_w and m_c, as well as on some functional relationship between gas saturation and the relative permeabilities k_{rl}, k_{rg}.

The mathematical problem of integration of the system of differential equations is a boundary value problem; the boundary conditions are just values of T and p_c. The system turns out to be stiff with respect to integration in the positive z-direction; most solutions are obtained by integration downwards. A fourth-order Runge-Kutta method was used, with a stepsize between 0.5 and 1 m providing stability and accuracy.

Some consideration was given to how the mass fluxes m_w and m_c might be determined. Four methods seemed possible:

(i) choose m_w and m_c independently (perhaps basing each on measured field values);

(ii) set a total mass flow $m_t = m_w + m_c$, and apportion m_w and m_c according to their total mobilities at the top of the heat pipe;

(iii) set a total mass flow m_t, and apportion m_w and m_c according to the total mass fraction of each at the top of the pipe;

(iv) set a total mass flow m_t, and apportion m_w and m_c according to the mass fraction of each in the gas phase only at the top of the pipe.

Each alternative has merit, depending on what mechanism is favored as a discharge condition at the top of the heat pipe. The results given below are calculated using (ii) but any of (i) - (iv) is easily implemented.

After all parameters are determined, or chosen, and relative permeability dependence on S_g is decided, integration of the equations proceeds. For given starting values of T and p_c, a solution for S_g and hence dT/dz and dp_c/dz is possible only provided q, m_w and m_c lie within a certain envelope. If so, there may be one or two solutions for S_g; if two, these correspond to the so-called vapor (gas)-dominated (larger S_g) or liquid-dominated (smaller S_g) heat pipes. In many cases, integration proceeds satisfactorily until a point is reached where there is suddenly no solution for S_g; this indicates a limit to the vertical extent of the heat pipe.

As can be seen, there are many parameters "to play with." Nevertheless, there are several characteristics that are common to most configurations studied so far; these are demonstrated in the examples chosen for illustration below.

RESULTS

The behavior of the two-component systems is best illustrated by considering some typical examples, and then making comparisons with them for other parameter values.

The most significant feature of most of the cases studied is the presence of a "wedge" of CO_2 partial pressure at the top of the system. This is demonstrated in Figure 1, where the variation with depth of total pressure, p, and CO_2 partial pressure, p_c, are plotted. At the top, T = 110 °C and p_c = 10 bar, with a net heat flux of 1 W/m^2 and various net total mass throughflows $m_t = 0$, 10^{-8} and 10^{-7} kg/m^2 s. The mass flows are apportioned to m_w and m_c according to the total mobilities at the top of the system. The relative permeability functions are chosen to be the Corey curves with residual liquid gas saturations $S_{lr} = 0.3$, $S_{gr} = 0.05$ respectively, while K = 2 W/m °C and k = 10^{-15} m^2 (1 md).

From the top of these systems, arbitrarily designated z = 0, the CO_2 partial pressure decreases while total pressure increases, albeit slowly in the case $m_t = 0$. For

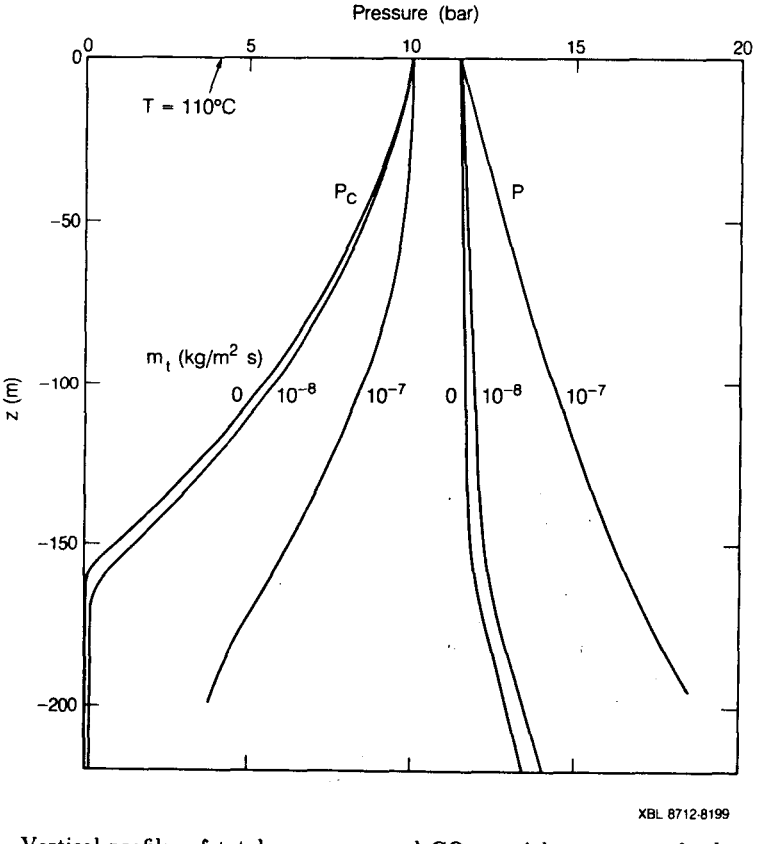

Figure 1. Vertical profiles of total pressure p and CO_2 partial pressure p_c for heat flow q = 1 W/m^2 and total mass throughflows $m_t = 0$, 10^{-8} and 10^{-7} kg/m^{2}s. Boundary conditions at the top are T = 110 °C and p_c = 10 bar. (K = 2W/m °C, k = 10^{-15} m^2, Corey relative permeabilities with $S_{lr} = 0.3$, $S_{gr} = 0.05$.)

that case ($m_t = 0$), p_c becomes almost zero at a depth of 160 m, and decays quickly below that point. For $m_t = 10^{-8}$, behavior is similar, but p_c does not become zero at depth because of the finite throughflow. For $m_t = 10^{-7}$, decrease of p_c is slower, and indeed there is no solution below 196 m, which corresponds to the limit of this two-phase heat transport mechanism. A system with single-phase water and dissolved CO_2 could be found to match the heat and mass flux requirements below this depth.

It should also be noted that it is possible, with suitable selection of q and m_t, to obtain pressure profiles where p_c increases significantly with depth. An example of such a profile was obtained as part of a simulation of Ohaaki by O'Sullivan et al. (1985). Such results are investigated further in McKibbin and Pruess (1988).

The three different pressure profiles in Figure 1 do not correspond to the same temperature profiles, although $T = 110\,^\circ C$ at the top of each. This and other such differences are also demonstrated in Figures 2 and 3, where a comparison between a vapor-dominated and a liquid-dominated heat and mass transfer mechanism is made. The top temperature is now $200\,^\circ C$, and the total mass throughflow is 10^{-8} kg/m^{2}s; otherwise parameters and relative permeability functions are as for Figure 1.

The profiles for temperature T, pressures p and p_c, gas saturation S_g, liquid flow rate $F_l = F_l^w + F_l^c$ and condensation rate (in kg/m^{3}s) are shown in Figures 2 and 3 for the vapor-dominated and liquid-dominated systems respectively. Both have a CO_2 partial pressure profile that decreases in a wedge shape to a very small value. Below this pressure transition point, the total pressure changes gradient slightly, increasing for the vapor-dominated, and decreasing for the liquid-dominated systems respectively. This opposite behavior is also reflected by the corresponding smooth but distinct changes in gas saturation at the base of the CO_2 gas wedge.

The liquid flow rate profiles indicate a very small value of F_l in the gas wedge region, with a significant condensation region at the base of the wedge. There is consequently very little mass counterflow taking place above the transition, with the main heat flow being conductive, as reflected by the temperature profiles: there is a nearly conductive gradient in the gas wedge region.

The overall effect of the gas wedge seems to be to provide a transition between the counterflow, or heat pipe, below and a conductive region above, with a short but significant condensation zone to accomplish this. Such provision of a condensation zone has not been noted before; most assumptions are based on condensation at an impermeable caprock.

The possibility of a mixed vapor-dominated/liquid-dominated heat transfer system is demonstrated in Figure 2, where dashed lines indicate the calculated profiles found by assuming that, below depths of 30 m, 60 m or 100 m, the system is liquid-dominated.

Comparison with MULKOM

Some comparisons were made between profiles calculated using Equations (1) - (7) as described above and results found by numerically running transient heat pipe conditions to steady state with the program MULKOM (Pruess, 1983). Over a simulated depth of 400 m, temperatures agreed to within $0.5\,^\circ C$ over a range of $100\,^\circ C$ and pressures to within 0.15 bars over a range of 6 bars with discretizations of both 20 blocks and 400 blocks for the MULKOM program. Since the correlations for the properties of water and CO_2, and the equation formulation are the same for both calculations, the small difference in results may be due to the consistent upstream weighting technique used in the transient calculations. Further investigation is proceeding.

Pressure/Throughflow Relationship at Great Depth

Substitution of Equations (1) - (4) into Equations (5) - (7) and subsequent elimination of k_{rl} and k_{rg} gives the following equation:

$$\rho_g \tau \phi S_g D_{vc} \frac{dY}{dz} = m_w Y + m_c (1 - Y)$$

$$+ (Y - X) \left[\frac{q + KT' - m_w h_g^w - m_c h_g^c}{(1 - X)(h_g^w - h_l^w) + X (h_g^c - h_l^c)} \right] \quad (8)$$

where $T' = dT/dz$. Provided m_w and m_c are not too large, calculations indicate that, below any gas wedge, Y does not vary much with depth; binary diffusion is therefore negligible in deeper regions, and can be neglected. Also, the assumption that the ideal gas law is satisfied closely, leads to a relationship between Y and p_c, namely

$$Y \approx \frac{p_c}{p_c + \rho_v R (T + 273.15)} \quad (9)$$

where $R = R_0/M_{CO_2} \approx 189$. Neglecting X, the very small mass fraction of CO_2 in the liquid flow, and substituting (9) into (8) with the LHS = 0 gives, upon rearrangement,

$$p_c \approx \frac{\rho_v R (T + 273.15) h_{lv}}{q + KT' - m_w h_l^w - m_c h_g^c} m_c \ .$$

For small mass fluxes, this reduces further to

$$p_c \approx \frac{\rho_v R (T + 273.15) h_{lv}}{q + KT'} m_c \quad (10)$$

which gives a simple approximate relationship between CO_2 partial pressure, p_c, and CO_2 mass flux per unit area, m_c. The proportionality coefficient depends only on the measured temperature and its gradient at a point (and, of course, an estimate of K and total heat transfer q, perhaps measured at the surface). Equation (10) may be useful in determining CO_2 mass fluxes from deep temperature and pressure profiles.

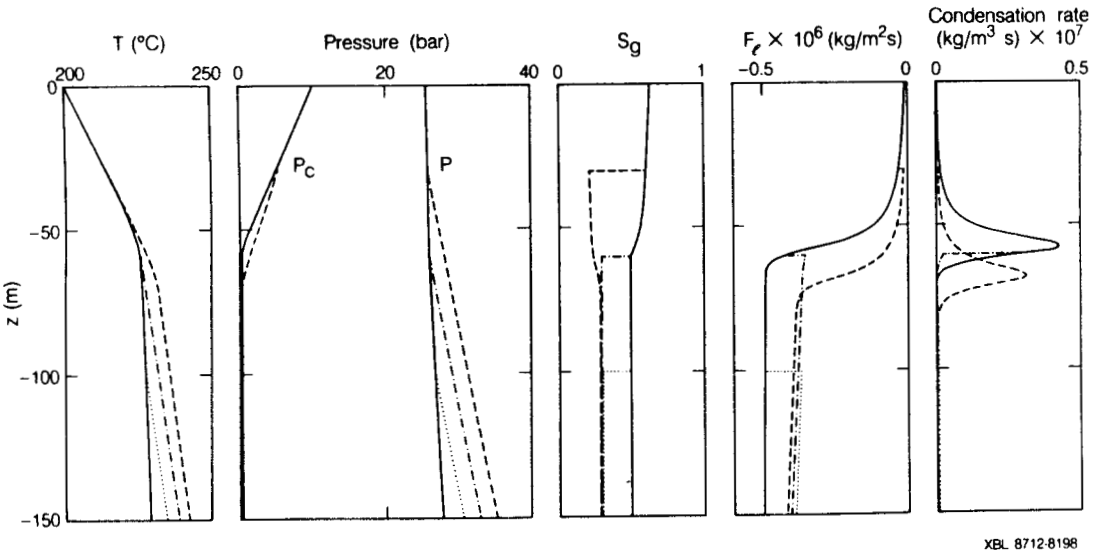

Figure 2. Vertical profiles of temperature T, pressures p and p_c, gas saturation S_g, liquid flow rate F_l and condensation rate for a vapor-dominated system with top conditions T = 200 °C and p_c = 10 bar. Total mass throughflow is 10^{-8} kg/m^{2}s. Other parameters are as for Figure 1. Broken lines correspond to liquid-dominated systems beneath the vapor-dominated system at depths of 30 m, 60 m or 100 m.

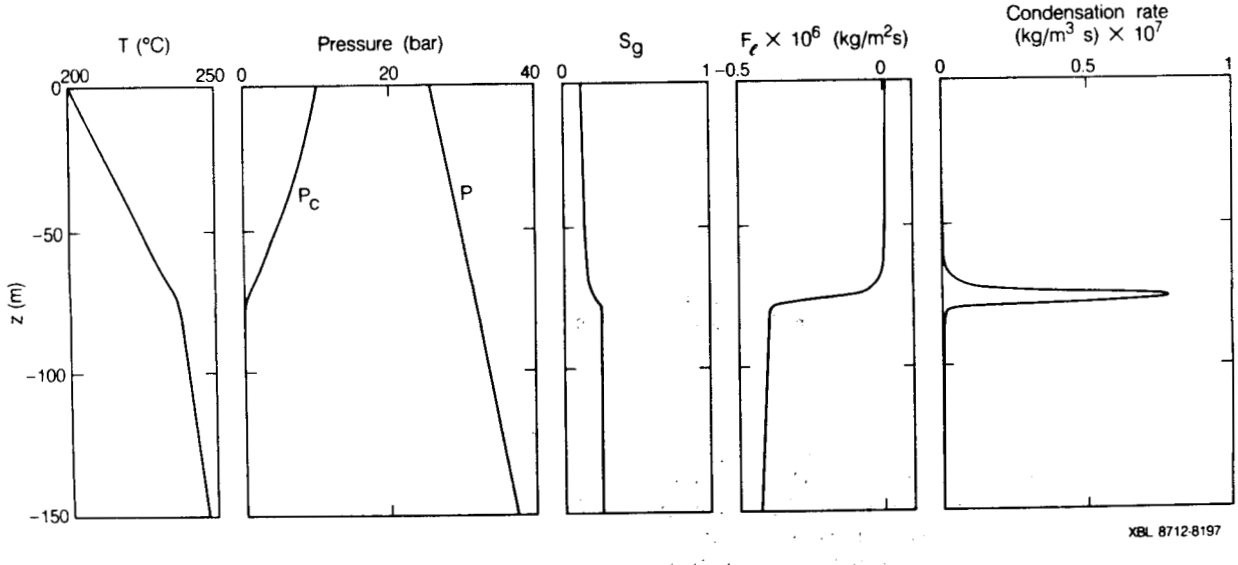

Figure 3. Vertical profiles of temperature T, pressures p and p_c, gas saturation S_g, liquid flow rate F_l and condensation rate for a liquid-dominated system. Parameters are as for Figure 2.

Inverse Problem

Writing

$$\overline{m} = \frac{q + KT' - m_w h_g^w - m_c h_g^c}{(1 - X)(h_g^w - h_l^w) + X(h_g^c - h_l^c)},$$

equation (8) may be rearranged to give an expression for $S_g \tau \phi$:

$$S_g \tau \phi = \frac{m_w Y + m_c (1 - Y) + \overline{m} (Y - X)}{\rho_g D_{vc} Y'}. \quad (11)$$

Use of (1) - (4) also gives expressions for kk_{rl} and kk_{rg} as follows:

$$kk_{rl} = \frac{\overline{m}}{(p' + \rho_l g)/\nu_l}, \quad (12)$$

$$kk_{rg} = \frac{(1 - X)\overline{m} + m_w - \rho_g S_g \tau \phi D_{vc} Y'}{-(1 - Y)(p' + \rho_g g)/\nu_g} \quad (13)$$

Theoretically, at least, expressions (11) - (13) enable values of $S_g \tau \phi$, kk_{rl} and kk_{rg} to be deduced from known (measured) values of q, m_w and m_c, an estimate of K, and measured values of temperature, pressure and their gradients at some depth in a reservoir (through correlations, all values of water and CO_2 properties and therefore X, Y and Y' can be subsequently calculated and substituted into (11) - (13)).

Preliminary investigations show that parameters can be estimated to within 10% from synthetic heat pipe data generated using the numerical solutions of the Equations (1) - (7) provided T, p are known to within 0.01 ° C and 0.01 bar respectively. These requirements are rather more stringent than current instrumentation would allow. Investigation is continuing to try to separate out the effects of accuracy of estimating absolute values of T and p from those of estimating the gradients. Results will be reported later (see McKibbin and Pruess, 1988). If reliable estimates can be made from Equations (11) - (13), then it should be possible to determine some relationship between phase saturations and relative permeabilities from field data. In any case, results to date show much better estimates coming from data within the gas wedge than from below it.

SUMMARY AND CONCLUSIONS

A model for steady-state vertical gravity-driven flows of two-phase mixtures of water and CO_2 has been presented. Numerical integration of the resulting differential equations gives vertical profiles of temperature, pressures, phase saturations and phase compositions.

In systems with relatively small mass throughflow the presence of CO_2 results in a "wedge" of CO_2 partial pressure at the top of the system. This decays to small, but finite pressures at depth for a non-zero CO_2 mass throughflow, and to zero pressure at depth for zero net throughflow. Within the gas pressure wedge, counterflow is small, and the counterflow (or coflow) heat transfer mechanism operating at depth is replaced by an almost conductive temperature profile. Between the two regions i.e. at the base of the wedge, a very active condensation zone controls the transition from heat pipe to conduction. Systems with significant throughflow of CO_2 display a different profile, with CO_2 partial pressure largest at depth.

From accurate observations of vertical pressure and temperature profiles the rate of CO_2 discharge may be estimated. Determination of in-place gas saturation, as well as effective liquid and gas phase permeabilities, is possible in principle; however the accuracy requirements for temperature and pressure measurements may be so stringent as to be impractical.

ACKNOWLEDGMENT

Robert McKibbin is grateful for the hospitality of the Earth Science Division, LBL, while taking part in this work during a period of sabbatical leave from the University of Auckland.

This work was supported through U.S. Department of Energy Contract No. DE-AC03-76SF00098.

NOMENCLATURE

a_{ij}, b_i	coefficients, functions of T, p_c, S_g
D_{vc}	binary diffusion coefficient (m^2/s)
F	mass flux per unit area (kg/m^2s)
g	gravitational constant (m/s^2)
h	specific enthalpy (J/kg)
h_{lv}	vaporization enthalpy for water (J/kg)
k	permeability (m^2)
k_{rl}, k_{rg}	relative permeabilities for liquid and gas phases
K	thermal conductivity of saturated formation (W/m ° C)
K_H	Henry's constant (Pa)
m	(constant) mass flux per unit area (kg/m^2s)
M_{H_2O}, M_{CO_2}	molecular weights of water and CO_2
p	pressure (Pa)
q	heat flux per unit area (W/m^2)
R	gas constant
S	saturation (volume fraction)
T	temperature (° C)
X	mass fraction of CO_2 in liquid phase
Y	mass fraction of CO_2 in gas phase
z	vertical coordinate (m)

Greek

ν	kinematic viscosity (m^2/s)
ρ	density (kg/m^3)
τ	tortuosity
ϕ	porosity

Super- and Subscripts

c	CO_2
g	gas
l	liquid
r	residual
t	total
v	vapor
w	water
0	standard value

REFERENCES

Atkinson, P. G., Celati, R., Corsi, R., and Kucuk, F., (1980), "Behavior of the Bagnore Steam/CO_2 Geothermal Reservoir, Italy," Soc. Petroleum Engineers J. (Aug. 1980), 228-238.

Iglesias, E. R., Arellano, V. M., and Ortiz-Ramirez, J., (1986), "Natural Vertical Flow in the Los Azufres, Mexico, Geothermal Reservoir," Proc. Eleventh Workshop on Geothermal Reservoir Engineering, Report SGP-TR-93, Stanford University, January 1986, 237-342.

Martin, J. C., Wegner, R. E., and Kelsey, F. J., (1976), "One-Dimensional Convective and Conductive Geothermal Heat Flow," Proc. Second Workshop on Geothermal Reservoir Engineering, Stanford University, 1976, 251-262.

McGuiness, M. J., and Pruess, K., (1987), "Unstable Heat Pipes," Proc. Ninth New Zealand Geothermal Workshop, University of Auckland, New Zealand, 1987.

McKibbin, R., and Pruess, K., (1988), "On Non-Condensible Gas Concentrations and Relative Permeabilities in Geothermal Reservoirs with Gas-Liquid Co- or Counterflows," in preparation.

O'Sullivan, M. J., Bodvarsson, G. S., Pruess, K., and Blakely, M. R., (1985), "Fluid and Heat Flow in Gas-Rich Geothermal Reservoirs," Soc. Petroleum Engineers J. (April 1985), 215-226.

Perry, J. H., (1963), "Chemical Engineers Handbook," McGraw-Hill, New York, Section 14, 19-23.

Pruess, K., (1983), "Development of the General Purpose Simulator MULKOM," Earth Sciences Division 1982 Annual Report, LBL-15500, Lawrence Berkeley Laboratory, Berkeley, CA, 133-135.

Pruess, K., (1985), "A Quantitative Model of Vapor-Dominated Geothermal Reservoirs as Heat Pipes in Fractured Porous Rock," Geothermal Resources Council Transactions 9 (August 1985), 353-361.

Pruess, K., Celati, R., Calore, C., and Cappetti, G., (1987), "On Fluid and Heat Flow in Deep Zones of Vapor-Dominated Geothermal Reservoirs," Proc. Twelfth Workshop on Geothermal Reservoir Engineering, Stanford University, 1987.

Straus, J. M., and Schubert, G., (1981), "One-Dimensional Model of Vapor-Dominated Geothermal Systems," J. Geophys. Res., 86, 9433-9438.

Sutton, F. M., and McNab, A., (1977), "Boiling Curves at Broadlands Geothermal Field, New Zealand," New Zealand J. Science, 20, 333-337.

Udell, K. S., and Fitch, J. S., (1985), "Heat and Mass Transfer in Capillary Porous Media Considering Evaporation, Condensation and Non-Condensible Gas Effects," Paper presented at 23rd ASME/AIChE National Heat Transfer Conference, Denver, CO, August 1985.

White, D. E., Muffler, L. J. P., and Truesdell, A. H., (1971), "Vapor-Dominated Hydrothermal Systems Compared with Water Systems," Economic Geology, 66, 75-97.